Electronic Supplementary Material (ESI) for RSC Advances.

The sorption of nonsteroidal anti-inflammatory drugs: diclofenac and naproxen onto UV and/or H_2O_2 treated MWCNT-COOH and MWCNT-OH

Bożena Czech*

Department of Environmental Chemistry, Faculty of Chemistry, Maria Curie-Skłodowska University, Pl. Marii Curie-Skłodowskiej 3, 20-031 Lublin, Poland

*corresponding author: e-mail@hektor.umcs.lublin.pl, phone +48 81 537 55 54, fax +48 81 537 55 65

Journal name: RSC Advances
Number of pages: 6
Number of tables: 4
Number of figures: 10
Date of preparation: September 2016.

Experimental

Chemicals and CNT

Diclofenac sodium ($C_{14}H_{10}Cl_2NNaO_2$, pKa 4.2) and naproxen ($C_{14}H_{14}O_3$, pKa 4.2) were purchased from Sigma-Aldrich (Poland). Multi-walled carbon nanotubes with -COOH groups (referred as CNTCOOH) and -OH groups (referred as CNTOH) were supplied by Timesnano, China. CNTs are characterized by >95% purity, 10-20 nm outer diameter and 10-30 μm length. The surface area (S_{BET}) of all studied materials was in the range of 159.1 to 208.8 $m^2 \cdot g^{-1}$.[1] The content of surface groups (XPS & Titration): -OH in CNTOH or -COOH in CNTCOOH was 3.06 wt% and 2.00 wt%, respectively. The procedure of CNT wastewater treatment was described in.[1] For the treatment of wastewater containing functionalized CNT, 0.35wt% addition of H_2O_2 (POCH, Poland) and/or 5 hours of UV irradiation (254 nm, 15 W) were applied. CNT after treatment were labeled as follows: CNTOH-UV or CNTCOOH-UV – indicating UV irradiated CNT; CNTOH-H_2O_2 or CNTCOOH-H_2O_2 – indicating H_2O_2 treatment of CNT and CNTOH-UV+H_2O_2 or CNTCOOH-UV+ H_2O_2 – indicating UV and H_2O_2 treatment.

Sorption models

The equilibrium sorption capacity was calculated using Eq. (1):

$$Q_e = \frac{(C_0 - C_e) * V}{m} \quad (1)$$

where Q_e is the equilibrium solid phase concentration of DCF or NPX ($mg \cdot g^{-1}$); C_o and C_e are the DCF/NPX concentrations of the initial and equilibrium aqueous phases ($mg \cdot L^{-1}$), respectively; V is the volume of solution (L), and M is the mass of adsorbent (g).

The Freundlich model describing sorption on heterogeneous surfaces, as well as multilayer sorption is expressed by Eq. (2):

$$Q_F = Q_F C_e^{1/n} \quad (2)$$

where Q_F is the relative adsorption capacity ($mg \cdot g^{-1}$), and n is a parameter related to linearity.

The sorption on planar surfaces and monolayer adsorption are described by the Langmuir model given by Eq. (3):

$$Q_L = \frac{Q_L K_L C_e}{1 + K_L C_e} \quad (3)$$

where Q_L is the maximum amount of DCF or NPX adsorbed ($mg \cdot g^{-1}$), and K_L is the sorption equilibrium constant ($L \cdot mg^{-1}$).

The essential features of the Langmuir model were expressed in terms of a separation factor (R_L) to determine whether the adsorption system was favorable or unfavorable in batch experiments, and is given by Eq. (4):

$$R_L = \frac{1}{(1 + K_L C_0)} \quad (4)$$

The Temkin model related to the heat of sorption is expressed by Eq. (5):

$$Q_T = \frac{RT}{b} ln(AC_e) \quad (5)$$

where R is the universal gas constant, T is the absolute temperature, b is the heat of adsorption, and A is the binding constant ($L \cdot mg^{-1}$).

The Dubinin–Radushkevich model describing sorption onto porous structure of the sorbent is given by Eq. (6):

$$Q_D = Q_D exp\left(-B_D\left[RT\ln\left(1 + \frac{1}{C_e}\right)\right]^2\right) \quad (6)$$

where Q_D is the adsorption capacity ($mg \cdot g^{-1}$), B_D is the mean free energy of sorption, and E is the bonding energy for the ion-exchange mechanism calculated using Eq. (7):[2]

$$E = \frac{1}{\sqrt{2B_D}} \quad (7)$$

Sorption kinetics

For the sorption of PPCPs there were applied 2 the most popular mathematical models of Lagergren and Ho-McKay (pseudo-first and pseudo-second order). The first order kinetics is described as follows (Eq. 9):

$$\log(Q_e - Q_t) = logQ_e - \frac{k_1}{2.303}t \quad (8)$$

where *Qe* and *Qt* are the amount of PPCPs sorbed at equilibrium and after time t (mg·g^{-1}). The value of k_1 was obtained from the linear relationship $log(Q_e - Q_t) = f(t)$ (Fig.S1-3, Fig. S6-8).
The pseudo-second order reaction is described (Eq. 10):

$$\frac{t}{Q_t} = \frac{1}{k_2 Q_e^2} + \frac{1}{Q_e} t \quad (9)$$

where k_2 (g·mg^{-1}·min^{-1}) is the adsorption rate constant of pseudo-second order adsorption rate. The k_2 values were obtained from the relations of t/Q_t vs. t.
Elovich (Eq. 10) and Intraparticle Diffusion models (IPD, Eq. 11).

$$\frac{dq}{dt} = \alpha e^{-\beta q_t} \quad (10)$$

$$q_t = k_{id}\sqrt{t} + C \quad (11)$$

where α is initial adsorption rate and β is the ratio between the surface coverage and the activation energy, K_{id} is the rate constant for intraparticle diffusion (mg·g^{-1} min$^{-1/2}$), *t* is the time (min), and *C* is intercept.[3]
PFO and PSO models described sorption under non-equilibrium conditions.[3] Elovich model describes chemical adsorption mechanism.[4] IPD model considers the external mass transfer from the solution to the liquid-solid interface and the diffusion inside the pores.[5]

Results and discussion

Table S1. The physicochemical properties of CNTOHs and CNTCCOHs.

Carbon nanotubes	S_{BET}	V_p	D_p	V_m	C	H	O	N	ID/IG	D_A	ζ	M
CNTOH	208.8	1.208	115.6	0.06306	96.49	0	3.055	0.46	1.05	1812.7	-13.12	-0.93
CNTOH-UV	176.7	1.173	132.7	0.05522	94.18	0.29	5.09	0.44	1.1	6383.7	-6.4	-0.45
CNTOH-H_2O_2	165.7	0.891	107.6	0.05115	96.11	0	3.47	0.415	1.18	5239.7	-8.06	-0.57
CNTOH-UV+H_2O_2	179	1.249	139.5	0.05377	97.43	0	2.145	0.425	1.28	1765.5	-8.5	-0.61
CNTCOOH	166.7	1.475	177	0.04997	94.51	0	5.01	0.485	1.17	1840.6	-16.05	-1.14
CNTCOOH-UV	179.2	1.135	126.7	0.05644	95.51	0	3.96	0.53	1.12	615.1	-4.14	-0.29
CNTCOOH-H_2O_2	159.1	1.012	127.2	0.05115	94.45	0.17	4.965	0.42	1.27	5968.6	13.22	0.94
CNTCOOH-UV+H_2O_2	167.1	1.1	131.7	0.05265	94.43	0.14	4.975	0.455	1.08	2640	8.65	0.61

S_{BET}- BET surface area – $m^2 \cdot g^{-1}$, V_p – pore volume – $cm^3 \cdot g^{-1}$, V_m – micropore volume – $cm^3 \cdot g^{-1}$, C,H,N,O – elemental composition – %, DA – aggregates diameter – nm, ζ - zeta potential - mV, M – mobility – $m^2 \cdot s^{-2} \cdot V^{-1}$

NPX

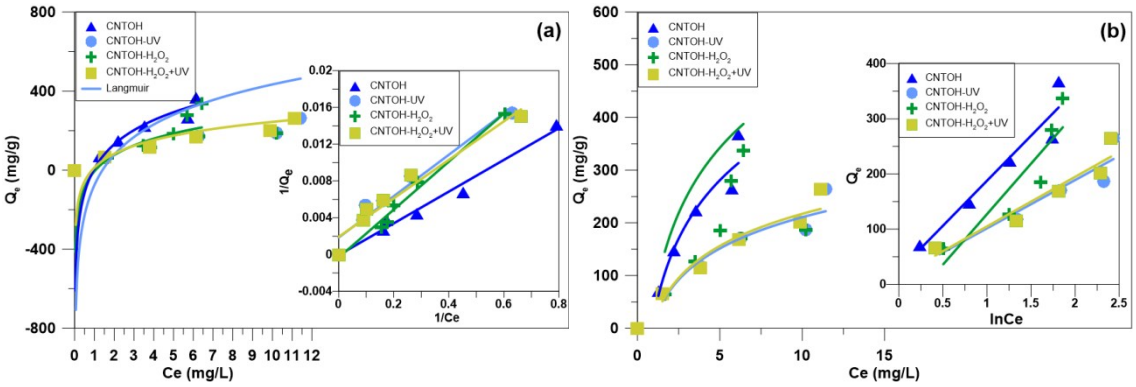

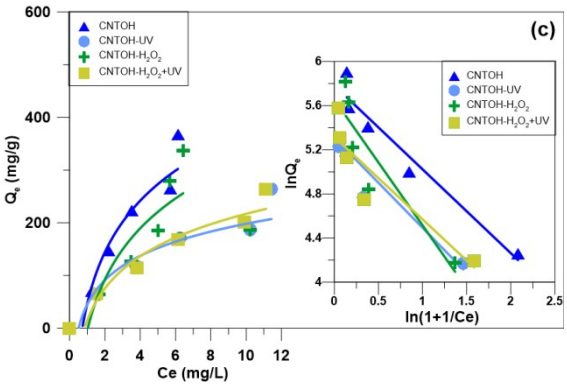

Fig. S1. The isotherm of NPX sorption over treated CNTOHs: (a) Langmuir, (b) Temkin, (c) Dubinin-Radushkevich. Lines represent the model predicted data fittings. Insets show the linearized form of adsorption isotherms.

Table S2. Linear parameters of Langmuir, Temkin and Dubinin-Radushkevich isotherms of NPX sorption over UV and/or H_2O_2 treated CNTOHs.

	Langmuir						Temkin				
	K_L	*STE*	Q_L	*STE*	R^2	$R_L \cdot 10^{-4}$	K_T	*STE*	*b*	*STE*	R^2
CNTOH	0,0325	0,0013	2000	76,950	0,1835	0,00005	1,162	0,045	163,22	6,28	0,9171
CNTOH-UV	0,1086	0,0018	416,667	6,782	0,7892	0,00024	1,173	0,019	87,463	1,42	0,8817
CNTOH-H_2O_2	0,0468	0,0004	714,286	5,982	0,4427	0,00014	1,357	0,011	182,94	1,53	0,8183
CNTOH-UV+H_2O_2	0,1	0,0032	454,545	14,580	0,8453	0,00022	1,183	0,038	89,82	2,88	0,9091

	Dubinin-Radushkevich				
	K_{DR}	*STE*	*E*	*STE*	R^2
CNTOH	$5 \cdot 10^{-8}$	$1{,}92 \cdot 10^{-9}$	0,1703	0,0066	0,8346
CNTOH-UV	$5 \cdot 10^{-8}$	$8{,}14 \cdot 10^{-10}$	0,1261	0,0021	0,8512
CNTOH-H_2O_2	$8 \cdot 10^{-7}$	$6{,}7 \cdot 10^{-9}$	0,0496	0,0004	0,8256
CNTOH-UV+H_2O_2	$1 \cdot 10^{-6}$	$3{,}21 \cdot 10^{-8}$	0,0419	0,0013	0,8234

K_L, K_{DR} - mg·g^{-1}, Q_L - L·g^{-1}, STE standard error

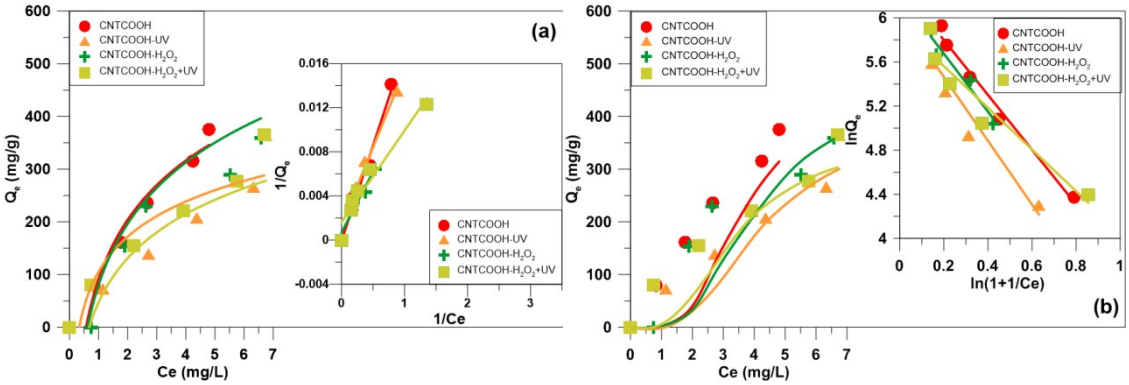

Fig. S2. The isotherm of DCF sorption over treated CNTCOOHs: a) Langmuir, b) Dubinin-Radushkevich. Lines represent the model predicted data fittings. Insets show the linearized form of adsorption isotherms.

Table S3. Linear parameters of Langmuir and Dubinin-Radushkevich isotherms of NPX sorption over UV and/or H_2O_2 treated CNTCOOHs.

	Langmuir						Dubinin–Radushkevich				
	KL	*STE*	*QL*	*STE*	R^2	*RL*	K_{DR}	*STE*	*E)*	*STE*	R^2
CNTCOOH	0.072	0.003	1428.6	55.0	0.8901	0.00007	$4 \cdot 10^{-7}$	$1 \cdot 10^{-8}$	0.039	0.001	0.9212
CNTCOOH-H_2O_2	0.743	0.012	384.6	6.3	0.8506	0.00026	$2 \cdot 10^{-6}$	$1 \cdot 10^{-8}$	0.119	0.002	0.1480

CNTCOOH-UV	0.050	0.000	1250.0	10.5	0.4258	0.00008	$6 \cdot 10^{-7}$	$1 \cdot 10^{-9}$	0.043	0.000	0.8278
CNTCOOH-H_2O_2+UV	0.177	0.006	588.2	18.9	0.8226	0.00017	$3 \cdot 10^{-7}$	$1 \cdot 10^{-9}$	0.043	0.001	0.8312

K_L, K_{DR} - mg·g^{-1}, Q_L - L·g^{-1}, E -kJ·g^{-1}, STE standard error

DCF

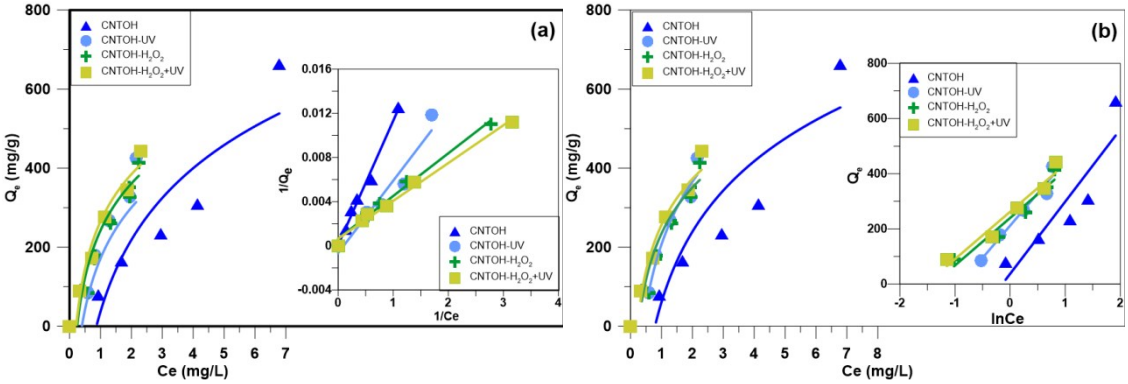

Fig. S3. The isotherm of DCF sorption over treated CNTOHs: (a) Langmuir, (b) Temkin. Lines represent the model predicted data fittings. Insets show the linearized form of adsorption isotherms.

Table S4. Linear parameters of Langmuir and Dubinin–Radushkevich isotherms of DCF sorption over UV and/or H_2O_2 treated CNTOHs.

	Langmuir						Dubinin–Radushkevich				
	K_L	*STE*	Q_L	*STE*	R^2	R_L	K_T	*STE*	*b*	*STE*	R^2
CNTCOOH	0.0043	0.000	20000	769.5	0.0067	0.000005	1.256	0.048	261.69	10.07	0.8175
CNTCOOH-H_2O_2	0.0667	0.001	2500	40.7	0.0743	0.000040	11.270	0.183	233.79	3.81	0.0594
CNTCOOH-UV	0.1795	0.002	1428.6	12.0	0.8919	0.000070	4.029	0.034	172.02	1.44	0.9453
CNTCOOH-H_2O_2+UV	0.2727	0.009	1111.1	35.6	0.8749	0.000090	4.611	0.148	171.51	5.50	0.952

K_L, K_t - mg·g^{-1}, Q_L - L·g^{-1}, STE standard error

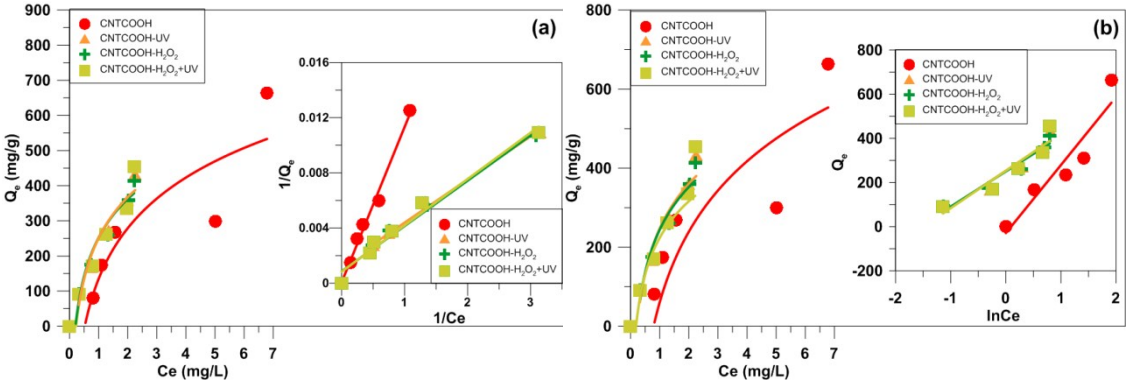

Fig. S4. The isotherm of DCF sorption over treated CNTOHs: (a) Langmuir, (b) Temkin. Lines represent the model predicted data fittings. Insets show the linearized form of adsorption isotherms.

Table S5. Linear parameters of Langmuir, Temkin and Dubinin-Radushkevich isotherms of DCF sorption over UV and/or H_2O_2 treated CNTCOOHs.

DCF	Langmuir						Temkin				
	K_L	*STE*	Q_L	*STE*	R^2	R_L	K_T	*STE*	*b*	*STE*	R^2
CNTCOOH	0.130	0.005	1111.11	42.8	0.3403	0.000090	1.954	0.075	205.95	7.92	0.7555
CNTCOOH-H_2O_2	0.333	0.005	909.09	14.8	0.9069	0.000110	4.811	0.078	159.12	2.59	0.9457
CNTCOOH-UV	0.257	0.002	1111.11	9.3	0.8445	0.000090	4.572	0.038	166.57	1.40	0.9332
CNTCOOH- H_2O_2+UV	0.250	0.008	1111.11	35.6	0.6651	0.000090	4.449	0.143	169.61	5.44	0.8894

K_L - mg·g^{-1}, STE standard error Q_L - L·g^{-1}, Q_D - mg·g^{-1}, E - kJ·g^{-1}

References

1 B. Czech, P. Oleszczuk and A. Wiącek, *Environ. Pollut.*, 2015, **200**, 161–167.

2 M. Ahmad, S. S. Lee, A. U. Rajapaksha, M. Vithanage, M. Zhang, J. S. Cho, S.-E. Lee and Y. S. Ok, *Bioresour. Technol.*, 2013, **143**, 615–622.

3 A. N. Módenes, F. R. Espinoza-Quiñones, A. Colombo, C. L. Geraldi and D. E. G. Trigueros, *J. Environ. Manage.*, 2015, **154**, 22–32.

4 F.-C. Wu, R.-L. Tseng and R.-S. Juang, *Chem. Eng. J.*, 2009, **150**, 366–373.

5 D. Kołodyńska, R. Wnętrzak, J. J. Leahy, M. H. B. Hayes, W. Kwapiński and Z. Hubicki, *Chem. Eng. J.*, 2012, **197**, 295–305.